Supplementary Material

Wolframite-type $MgReO_4$ under pressure: An experimental and theoretical study

Sinhué López-Moreno,*,† Neha Bura,¶ Pablo Botella,¶ Catalin Popescu,§ and Daniel Errandonea*,¶

†*División de Materiales Avanzados-IPICYT/SECIHTI, Camino a la presa de San José 2055 Col. Lomas 4a sección, San Luis Potosí 78216, México*

‡*Grupo de Ciencia e Ingeniería Computacionales-Centro Nacional de Supercómputo, IPICYT, Camino a la presa de San José 2055 Col. Lomas 4a sección, San Luis Potosí 78216, México*

¶*Departamento de Física Aplicada-ICMUV, MALTA Consolider Team, Universidad de Valencia, Dr. Moliner 50, Burjassot, 46100 Valencia, Spain*

§*CELLS-ALBA Synchrotron Light Facility, Cerdanyola, 08290 Barcelona, Spain*

E-mail: sinhue.lopez@ipicyt.edu.mx; daniel.errandonea@uv.es

Contents

1 Description

In this **Supplementary Material**, the theoretical results calculated without spin-orbit coupling are presented, which cause a distortion of the crystal structure at high pressure, affecting the vibrational properties of $MgReO_4$.

2 Computational Details

Total-energy calculations have been performed within the framework of the density functional theory (DFT)[1] and the projector-augmented wave (PAW)[2,3] method as implemented in the Vienna *Ab initio* Simulation Package (VASP).[4] We have considered six valence electrons for O atoms ($2s^2$, $2p^4$), thirteen for Re ($5p^6$, $5d^5$, $6s^2$), and eight for Mg ($2p^6$, $3s^2$) in the PAW pseudo-potential. We have used a plane-wave energy cutoff of 520 eV to ensure high precision in our calculations. The exchange-correlation energy has been described within the generalized-gradient approximation (GGA) in the Perdew-Burke-Ernzerhof for solids (PBEsol) formulation.[5]

The Monkhorst-Pack scheme has been employed for the Brillouin-zone (BZ) integrations[6] with a mesh 4×4×4, which corresponds to a set of sixteen special k-points in the irreducible

BZ. In the relaxed equilibrium configuration, the forces are less than one meV/Å per atom in each Cartesian direction. The highly converged results on forces are required to calculate the dynamical matrix using the direct force constant approach.[7] This allows us to identify the irreducible representation and the character of the phonon modes at the zone center (Γ point).

3 Structural parameters

According to Fig. 1 (b), the theoretical lattice parameter a is very similar to the experimental one. However, our calculations' lattice parameters b and c present a deviation from the experimental results around ≈10 GPa. The change in b and c lattice parameters originated from a distortion of the ReO_6 octahedra in the xy plane is due to abrupt changes in the angles of interatomic distances d_2 and d_3 inside the ReO_6 octahedra, see the inset of Fig. 2 (d). Such distortion is responsible for the abrupt change in the β angle, as seen in the inset of Fig. 1 (a). However, despite the change in interatomic distances, there is no appreciable change in the polyhedral volume of the ReO_6 octahedra [V_{ReO_6}, Fig. 2 (a)] but an increase in the distortion parameter (Δ_d) of both polyhedra.

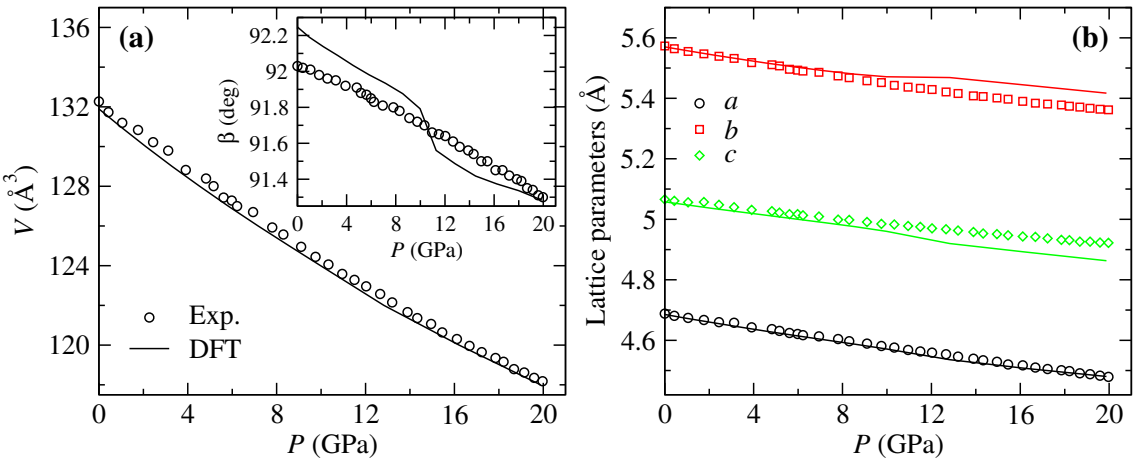

Figure 1: Pressure evolution of (a) unit-cell volume and β angle in the inset; (b) unit-cell lattice parameters of $MgReO_4$. Symbols correspond to experiments and solid lines to results from calculations.

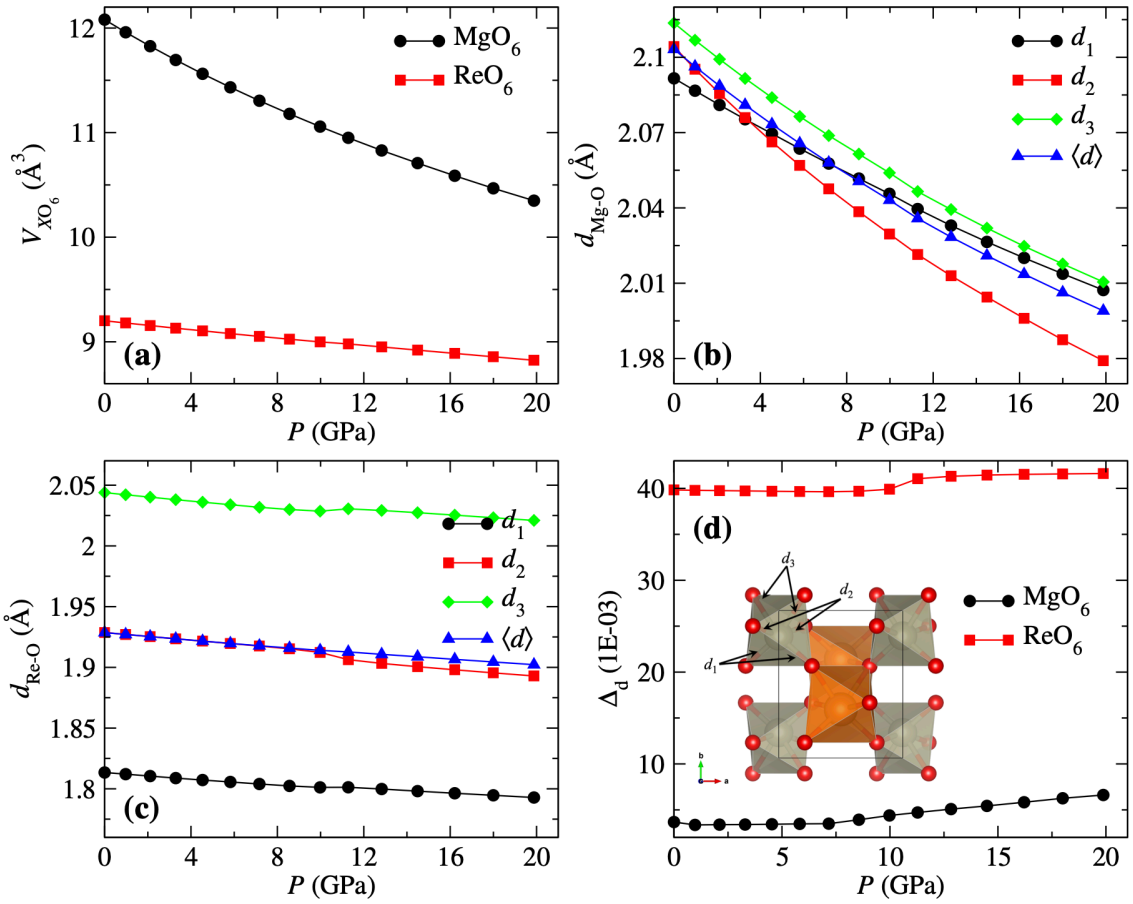

Figure 2: Structural parameters of $MgReO_4$ as a function of pressure: (a) polyhedral volumes V_{MgO_6} and V_{ReO_6}, interatomic distances (d_x) inside the (b) MgO_6 and (c) ReO_6 distorted octahedra, and (d) distorted parameter Δ_d. The inset of (d) shows the interatomic distances responsible for the distortion at ≈10 GPa.

To understand the origin of the distortion within this methodology without spin-orbit coupling, we performed several calculations fixing the β angle and the lattice parameters b and c to the low-pressure trend. Our results show that, under these conditions, the crystal structure is subjected to non-hydrostatic stress, resulting in an energy change of 3 meV/f.u.

4 Vibrational properties

The phonon frequencies computed with the direct force constant approach[7] at ambient pressure (in cm^{-1}), their pressure coefficients ($d\omega/dP$, in cm^{-1}/GPa), and the Grüneisen parameters (γ) are listed in Table 1. Where $d\omega/dP$ and γ were obtained from ambient pressure

up to 10 GPa in order to avoid the changes due to the structural distortion observed at ≈10 GPa. The pressure evolution of the Raman and infrared phonon frequencies appear in Fig. 3 (a) and (b), respectively. As can be seen, the Raman modes are more affected by the distortion of the crystalline structure at ≈10 GPa.

Table 1: Computed Raman and infrared phonon frequencies (ω, in cm^{-1}) of $MgReO_4$ at the Γ point and ambient pressure. We also included the pressure coefficients ($d\omega/dP$, in cm^{-1}/GPa) and the Grüneisen parameters (γ). $d\omega/dP$ and γ were computed in the pressure range 0-10 GPa.

	Raman				Infrared		
	ω	$d\omega/dP$	γ		ω	$d\omega/dP$	γ
B_g	116.85	0.13	0.17	B_u	176.96	0.73	0.71
A_g	183.64	-0.07	-0.06	B_u	234.37	-1.04	-0.80
B_g	191.41	0.29	0.24	A_u	253.79	1.22	0.82
B_g	225.97	0.49	0.34	B_u	267.43	-0.63	-0.43
B_g	241.61	2.25	1.40	A_u	307.43	0.33	0.19
B_g	273.40	1.06	0.60	B_u	311.26	3.43	1.77
A_g	280.97	-0.98	-0.54	B_u	326.51	4.58	2.19
A_g	293.35	2.28	1.18	A_u	345.09	1.03	0.52
A_g	345.82	4.51	1.93	A_u	414.94	4.28	1.66
B_g	346.59	4.69	2.00	B_u	462.98	5.31	1.83
A_g	399.10	1.17	0.45	A_u	494.80	4.06	1.34
B_g	403.87	4.48	1.66	B_u	540.73	3.75	1.15
B_g	514.38	3.10	0.92	A_u	619.43	3.99	1.07
A_g	552.58	2.52	0.70	B_u	731.74	3.68	0.85
B_g	631.17	4.63	1.11	A_u	753.26	2.95	0.67
A_g	671.60	3.27	0.74				
B_g	732.18	4.60	0.96				
A_g	873.35	4.41	0.77				

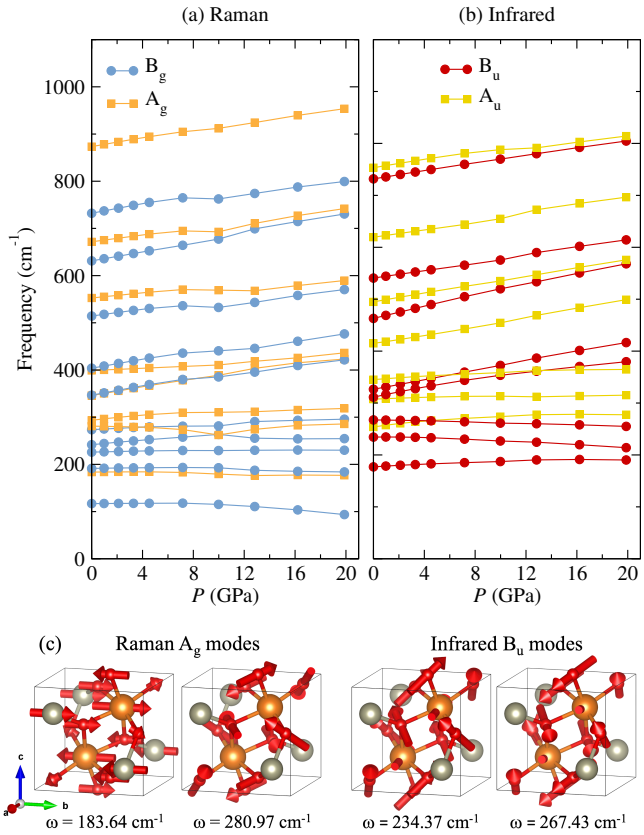

Figure 3: Pressure dependence of the (a) Raman and (b) infrared phonon frequencies of $MgReO_4$. (c) Lattice vibrations at ambient pressure of phonon frequencies with negative phonon pressure coefficients at the Γ point, see Table 1.

References

(1) Jones, R. O. Density functional theory: Its origins, rise to prominence, and future. *Rev. Mod. Phys.* **2015**, *87*, 897–923, DOI: https://doi.org/10.1103/RevModPhys.87.897.

(2) Blöchl, P. E. Projector augmented-wave method. *Phys. Rev. B* **1994**, *50*, 17953–17979, DOI: https://doi.org/10.1103/PhysRevB.50.17953.

(3) Kresse, G.; Joubert, D. From ultrasoft pseudopotentials to the projector augmented-wave method. *Phys. Rev. B* **1999**, *59*, 1758–1775, DOI: https://doi.org/10.1103/PhysRevB.59.1758.

(4) Kresse, G.; Furthmüller, J. Efficient iterative schemes for *ab initio* total-energy cal-

culations using a plane-wave basis set. *Phys. Rev. B* **1996**, *54*, 11169–11186, DOI: https://doi.org/10.1103/PhysRevB.54.11169.

(5) Csonka, G. I.; Perdew, J. P.; Ruzsinszky, A.; Philipsen, P. H. T.; Lebègue, S.; Paier, J.; Vydrov, O. A.; Ángyán, J. G. Assessing the performance of recent density functionals for bulk solids. *Phys. Rev. B* **2009**, *79*, 155107, DOI: https://doi.org/10.1103/PhysRevB.79.155107.

(6) Monkhorst, H. J.; Pack, J. D. Special points for Brillouin-zone integrations. *Phys. Rev. B* **1976**, *13*, 5188–5192, DOI: https://doi.org/10.1103/PhysRevB.13.5188.

(7) Parlinski, K. Computer Code PHONON. See: http://wolf.ifj.edu.pl/phonon, 2008.